Synthesis of Chromophores with Extremely High Electro-optic Activities. 2. Isophorone- and Combined Isophorone–Thiophene-Based Chromophores

Mingqian He,* Thomas M. Leslie, John A. Sinicropi, Sean M. Garner, and Leon D. Reed

Corning Incorporated, SP-FR-6, Corning, New York 14831

Received April 22, 2002. Revised Manuscript Received September 3, 2002

Four new isophorone and combined isophorone and thiophene bridged chromophores have been synthesized. All of these new high $\mu\beta$ chromophores possess our newly synthesized tricyanovinyldihydrofuran acceptors. Because of our unique acceptor design, all of our chromophores show high solubility in all organic solvents due to minimized chromophore–chromophore electrostatic interactions. These chromophores have also been studied with respect to their solvatochromism and thermal behavior by TGA in air. Preliminary EO characterization of one of these chromophores in polycarbonate has demonstrated an extremely high r_{33} of 70 pm/V at 1550 nm. We believe that this is the largest r_{33} reported at this wavelength.

Introduction

We report here the synthesis of several new high $\mu\beta$ electro-optic (EO) chromophores and, for one compound, characterization of the r_{33} value through contact poling. Recently, significant progress has been made in the synthesis and subsequent processing of these new materials into high-speed devices.[1,2] Devices using these newly reported high $\mu\beta$ chromophores have brought polymer EO devices to the brink of commercialization. With the renewed interest in organic-based EO materials, even more new high $\mu\beta$ chromophores with unique structures have been developed, showing even higher electro-optic (EO) coefficients.[3] But to be accepted for use in a commercial device, organic NLO materials must meet very stringent environmental requirements. High electro-optic activity is not the only criterion for use in a device format; it must also show good thermal and photochemical stability. The host material must possess optical transparency at communication wavelengths. It also must include the ability to maintain the aligned chromophores in a noncentrosymmetric fashion after poling and maintain its high EO coefficient. Theoretical calculations and experimental results have born out that high $\mu\beta$ chromophores are difficult to align due to the chromophore's high ground-state dipole moment interactions.[3] Preventing chromophore–chromophore antiparallel interaction at the molecular level should lead to significant improvement of the poling process and therefore achieve the necessary high EO coefficients. To minimize this antiparallel packing, the nondendrimeric chromophores reported to date have been designed with floppy side chains attached to the flat conjugated structure. This approach seems to be successful based on the latest published data for what are known as the CLD and FTC type of chromophores[4,5] (Figure 1).

An alternative approach that has proven to be efficient in preventing chromophore antiparallel packing is the use of dendrimeric structures that bury the chromophore inside, physically separating them with bulky chains.[6] Previously, we published in this journal a series of bulky three-dimensional tricyanovinyldihydrofuran type of acceptors[7] (Figure 2).

The intent of this work is that when R_1 and R_2 are both above and below the chromophore's plane of conjugation, we should significantly increase the solubility and decrease the chromophore dipolar packing. To test this hypothesis further, we have designed various donor bridges to couple with our acceptors, making several new novel chromophores. It has been reported that the CLD type of chromophores have exhibited some solubility problems.[8] Our conjecture is crystallization occurs due to the strong ground-state dipole moment induced by the very flat (when R_1 and R_2 are methyl) tricyanovinyldihydrofuran (TCF) acceptor being incorporated into a larger rigid flat structure. The CLD type of structure with the isophorone-based bridge does not have the bulky alkyl groups in the center to help prevent crystallization. By modification of the TCF type of acceptor, we have been able to overcome

(1) Chen, D.; Fetterman, H. R.; Chen, A.; Steier, W. H.; Dalton, L. R.; Wang, W.; Shi, Y. *Appl. Phys. Lett.* **1997**, *70*, 3335.
(2) Shi, Y.; Zhang, C.; Zhang, H.; Bechtel, H. J.; Dalton, L. R.; Robinson, B. H.; Steier, W. H. *Science* **2000**, *288*, 119.
(3) Dalton, L. R. *Opt Eng.* **2000**, *39* (3), 589.
(4) Wang, F.; Ren, A. S.; He, M.; Harper, A. W.; Dalton, L. R.; Garner, S. M.; Zhang, H.; Chen, A.; Steier, W. H. *Polym. Mater. Sci. Eng.* **1998**, *78*, 42.
(5) Zhang, C.; Ren, A. S.; Wang, F.; Dalton, L. R. *Polym. Prepr.* **1999**, *40*, 49.
(6) Ma, H.; Chen B.; Sassa, T.; Dalton, L. R.; Jen, K.-Y. Alex. *J. Am. Chem. Soc.* **2001**, *23*, 986.
(7) He, M.; Leslie, M. T.; Sinicropi, J. A. *Chem. Mater.* **2002**, *14* (5), 2393.
(8) Zhang, C.; Dalton, L. R.; Oh, M.; Zhang, H.; Steier, W. H. *Chem. Mater.* **2001**, *13*, 3043.

10.1021/cm0204066 CCC: $22.00
Published on Web 10/15/2002

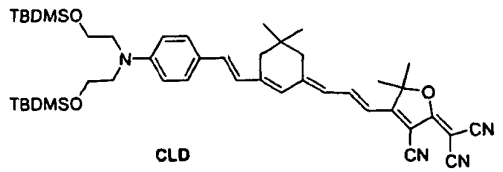

Figure 1.

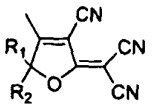

Figure 2. General acceptor structure.

Scheme 1. Synthesis of Acceptors

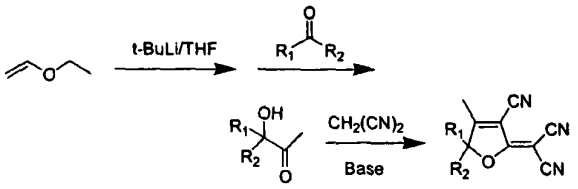

this problem. When comparing our chromophores to CLD, we found that all of our chromophores can be easily doped into polycarbonate (PC) up to about 35 wt % chromophore level or even higher. We also are able to eliminate the bulky *tert*-butyldimethylsilyl (TBDMS) groups from our chromophores, which are known to aid solubility of high $\mu\beta$ chromophores in doped polymer systems. By elimination of the TBDMS groups, the C−H bond count is significantly decreased, possibly lowering the optical loss at communication wavelengths.

Results and Discussions

Our synthetic approach for making new chromophores is based on our unique acceptors.[7] Previously, we reported the synthesis of these novel acceptors; included here is a brief overview of the synthesis shown in Scheme 1.

Models of the acceptors we have synthesized show that R_1 and R_2 are both well out of the conjugation plane of the furan structure. We intentionally designed our acceptors to have R_1 and R_2 very different with respect to each other, the concept being that a large size difference will make the chromophore more soluble. It is clear there is a chiral center at the carbon shared by R_1 and R_2 and we believe by not resolving the enantiomers, it results in better solubility of the chromophore in solvents and, more importantly, the polymer matrix. Of course, we plan to investigate the effects associated with a chiral center when a pure enantiomer is incorporated into a chromophore. We currently are separating optically pure chiral acceptors and will publish the results when available. The acceptor structures used in this study are listed in Figure 3. The chromophores were synthesized based on two different donor bridge systems.

One set is aminobenzene donor and isophorone bridge-based chromophores as compared to the aminobenzene donor and thiophene bridge compounds outlined in part 1 of this study.

Replacing the thiophene ring bridge with a polyene or ring-locked polyene such as isophorone has been

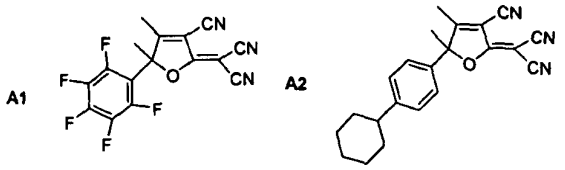

Figure 3. Acceptors.

shown to result in dramatic increases of the molecular nonlinearity.[9,10] However, there are some drawbacks when this substitution takes place. The most obvious disadvantage of a polyene bridge is lower chromophore thermal stability as observed through TGA testing in air. When a ring-locked structure is compared to a polyene, the molecular nonlinearity tends to decrease, but thermal stability tends to increase.[11,12] This will be addressed in detail in a later section. Two isophorone only bridge-based chromophores were synthesized to directly compare a thiophene-based bridge with isophorone-based bridges.[14] Because of our unique acceptor designs, our chromophores were not found to have solubility problems.

The synthesis of this type of chromophore was conducted as shown in Scheme 2.

Compound **2** was synthesized following a recent reference.[13] No matter which synthetic method was chosen in our laboratories, compound **3** was always obtained as a cis−trans isomer mixture. Details concerning the amounts of trans and cis isomers have been reported by Zhang et al.[8]

The second type of compounds are aminobenzene donor, isophorone−thiophene double-bridge-based chromophores.

Previously, Jen and co-workers[15] reported the synthesis of a long conjugated chromophore containing an isophorone−thiophene combination bridge. It is expected that when the overall conjugation length has been extended, the chromophore should have a larger $\mu\beta$ value. Also, it is expected that by extension of the conjugation length, the chromophore solubility will decrease significantly. We have found that with a modified thiophene bridge and our very anisotropicly shaped acceptors we were able to prepare two soluble chromophores containing both isophorone and thiophene units as a combination bridge shown in Figure 4. This good overall solubility allowed us to investigate in more detail the effects of conjugation length.

The synthesis of chromophores **6** and **7** are based on our previously described intermediates.[14] Compounds **1** and **3** were used to react with compound **8** in $NaOC_2H_5$ /HOC_2H_5 solution. These intermediates were then further reacted with butyllithium/DMF to prepare

(9) Ahlheim, M.; Barzoukas, M.; Besworth, P. V.; Blanchard-Desce, Fort, A.; Hu, Z−y.; Marder, S. R.; Perry, J. W.; Runser, C.; Staehelin, M.; Zysset, B. *Science* **1996**, *271*, 335.
(10) Marder, S. R.; Cheng, L. P.; Tiemann, B. C.; Friedli, A. C.; Blanchard-Desce, M.; Perry, J. W.; Shindhoj, J. *Science* **1994**, *263*, 511.
(11) Shu, C. F.; Shu, Y. C.; Gong, Z. W.; Peng, S. M.; Lee, G. H.; Jen, A. K.-Y. *Chem. Mater.* **1998**, *10*, 3284.
(12) Beritung E. M.; McMahon, R. J. *Mater. Res. Soc. Symp. Proc.* **1999**, *561*, 39.
(13) Spangler, C. W.; He, M. *J. Chem. Soc., Perkin Trans 1* **1995**, 715.
(14) He, M.; Leslie, M. T.; Sinicropi, J. A. *Chem. Mater.* **2002**, *14*, 4662−4668.
(15) Shu, C. F.; Tsai, W. J.; Chen, J. Y.; Jen, A. K. Y.; Zhang, Y.; Chen, T. A. *Chem. Commun.* **1996**, 2279.

Scheme 2

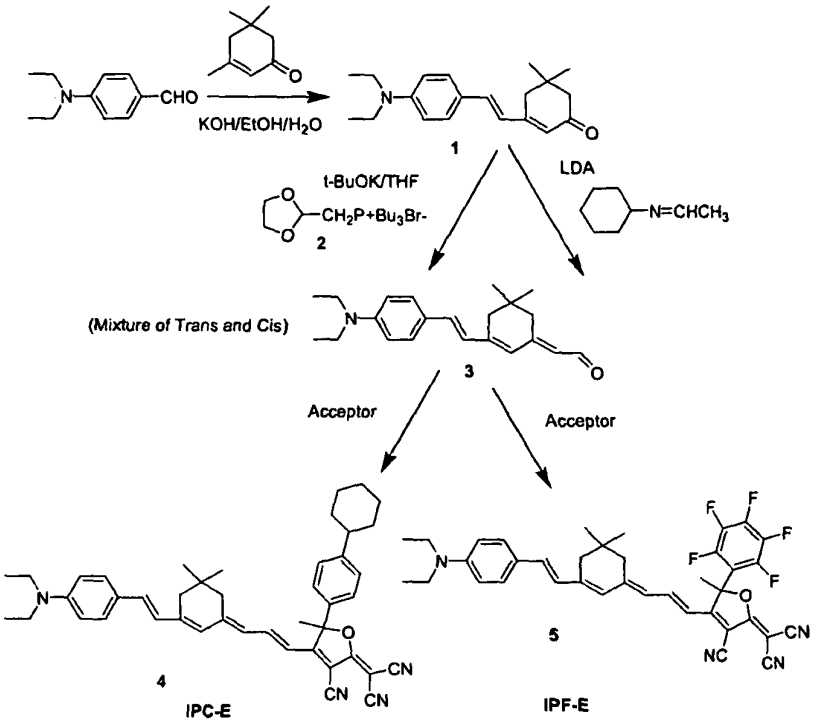

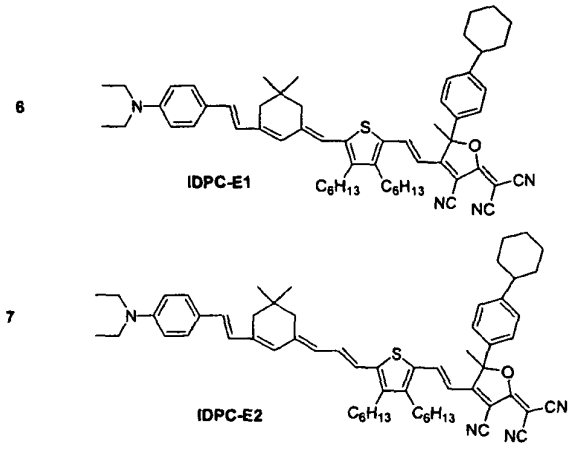

Figure 4. Isophorone and thiophene double-bridge based chromophores.

the corresponding aldehydes. These aldehydes were easily coupled with our acceptors to form the chromophores (Scheme 3).

UV–Vis–NIR Studies of the Chromophores. All of our chromophores can be dissolved into both chloroform and toluene; the absorption spectra have been obtained in both solvents to determine the wavelength of the maximum absorption of the charge-transfer band. The chromophores were also given letter names in our laboratory to simplify identification within the group. All of the names along with the corresponding compound numbers are included in Table 1.

Again, as found in part 1, longer conjugation length does not always lead to a greater solvatochromic energy shift. Chromophores **4** and **5** both have an isophorone bridge that a previous reference has mentioned to as essentially a locked diene bridge.[8] This type of bridge tends to result in higher $\mu\beta$ chromophores when comparing them to an aromatic bridge-based chromophore such as thiophene. The UV data show that **4** and **5** are red-shifted 50 and 60 nm, respectively, to their thiophene bridge counterparts.[14] We also believe that the pentafluorophenyl-based acceptor is not a much stronger acceptor since even though λ_{max} of **5** with the pentafluorophenyl moiety is 55-nm red-shifted when compared to **4** with the hydrocarbon moiety for both solvents the energy difference is the same. Compounds **6** and **7** have the longest conjugation length among our entire set of chromophores but not substantially higher energy changes. The combination isophorone–thiophene double-ring bridges seems to be too long for effective charge transfer through the entire chromophore π system. Compound **6** has its maximum absorption at 742 nm with an additional peak at 389 nm, while **7** has its maximum absorption at 760 nm and an additional peak at 407 nm as shown in Figure 5. Both of these additional absorption peaks at 389 and 407 nm appear at shorter wavelengths for both solvents, an effect not seen for any of the other compounds. We believe the charge transfer through the π system from end to end is not complete with some charge remaining on the aromatic thiophene ring creating the shorter wavelength absorption peak. The UV–Vis spectrum of the donor double-bridge compound **9** seems to verify our assumption having its absorption maximum at the same wavelength, 400 nm, that the new absorption peak appears.

It is well-known that solvatochromic effects are indicative of the chromophore's $\mu\beta$ value and several recent review articles have been written on the subject.[16,17] On the basis of simple solvent studies using polar chloroform and less polar toluene, we found that

Scheme 3

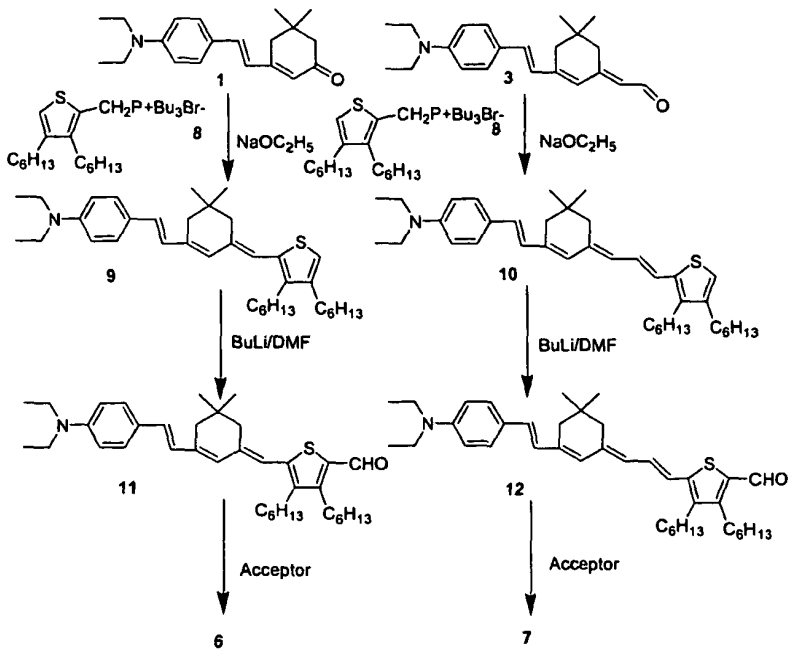

Chromophore 7 in Chloroform

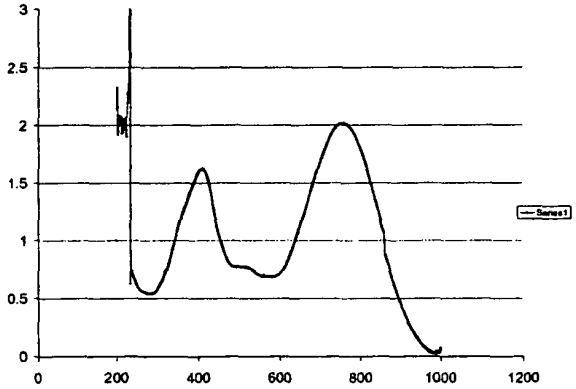

Figure 5. UV spectra of chromophore 7 in chloroform.

Table 1. Maximum Absorption of Chromophores

compd	chloroform (nm)	λ_{max} (cm^{-1})	toluene (nm)	λ_{max} (cm^{-1})	change (eV)	lab. name
4	705.8	14 168.3	664.9	15039.8	0.108	IPC-E
5	760.2	13 154.4	713.1	14023.3	0.108	IPF-E
6	742.1	13 475.3	702.7	14230.8	0.094	IDPC-E1
	389.4		389.4			
7	760.2	13 154.4	722.2	13846.6	0.086	IDPC-E2
	407.6		413.5			
9	407.6		407.0		N/A	N/A

chromophores **4** and **5** show the largest energy shift of the charge-transfer band (0.108 eV) while the longer chromophores **6** and **7** have 0.094 and 0.086 eV changes, respectively. It was also noted that TBDMS, used to protect the hydroxy functions on the chromophores, shows a bigger change in the charge-transfer band when compared to the analogous hydroxyl-containing chromophores.[14]

Table 2. TGA Test of Chromophore Thermal Stability

chromophore	lab. name	5% weight loss (°C)	melting point (°C)
4	IPC-E	270.3	214–216
5	IPF-E	251.6	180–182
6	IDPC-E1	264.9	118–120
7	IDPC-E2	291.0	134–136

Thermal Stability of Chromophores. TGA testing of the chromophores has been performed in an air atmosphere. The test results are listed in Table 2 and the results are shown in Figures 5 and 6.

Comparing the onset of weight loss of chromophores **4**–**5** from Figure **5**, we found **4** to be much more stable since **4** begins to decompose around 200 °C, where **5** begins thermal decomposition around 100 °C. We believe this is caused by the strong electron withdrawal of the pentafluorophenyl ring-containing acceptor; being a good leaving group, this corresponds to our previous hypothesis since we noticed the same behavior in our thiophene-based chromophores in a previous study.[14] Figure 6 clearly shows that **5** begins to decompose much earlier than its hydrocarbon counterpart.

At this time we do not have clear mechanistic evidence for this behavior but we think it is due to the following reasons. (1) The strong electron-withdrawing pentafluorophenyl ring causes the furan structure to be unstable with respect to either ring opening or a pentafluorophenyl radical leaving group, resulting in easier decomposition. (2) We know that the additional electron-withdrawing ability has made a large (55 nm) red shift in the chromophore's absorption peak, lowering the energy levels of the HOMO and LUMO which may facilitate molecular rearrangements. (3) Because fluorine withdraws electron density so strongly, the fluorinated benzene ring may separate from the tricyanofuran ring-forming radicals that further decompose. Chro-

(16) Nigam, S.; Rutan, S. *Appl. Spectrosc.* **2001**, *55*, 362A–370A.
(17) Painelli, A.; Terenziani, F. *Chem. Phys. Lett.* **1999**, *312*, 211–220.

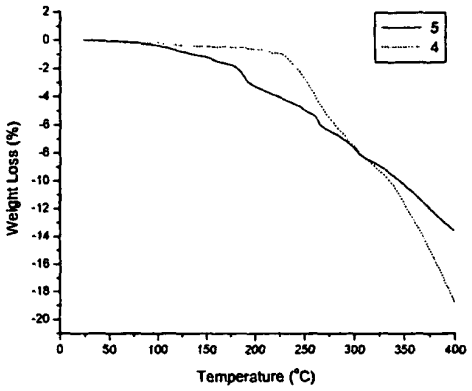

Figure 6. TGA of chromophores **4** and **5**.

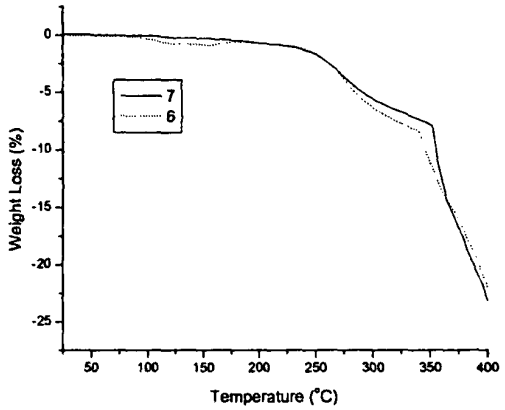

Figure 7. TGA of chromophores **6** and **7**.

mophores **6** and **7** both have an isophorone–thiophene double-ring bridge. We initially thought that these two compounds would be the least thermally stable of the set due to their extremely long conjugation length. But TGA tests in air have shown that they both are very stable with respect to breaking into smaller fragments as seen in Figure 7. The 5% weight loss by TGA is 264.9 °C for **6** and 291.0 °C for **7**.

Electro-optic Characterization. We selected **4** as the first chromophore on which to evaluate the electrooptic coefficient since it has the most pronounced "fishhook" shape. This shape was expected to give high solubility and low chromophore–chromophore pairing, facilitating poling. Evaluation of the chromophore nonlinear strength consisted of the following procedure. First, the chromophore was doped at 35 wt % into purified polycarbonate (Aldrich poly[Bisphenol A carbonate-*co*-4,4′-(3,3,5-trimethylcyclohexylidene)diphenol carbonate]). 35% chromophore loading was used based on observing no haze in cast films prior to poling; at higher concentrations the films became hazy. Solutions of 10% total solids were prepared in 1,2-dichloroethane and 3–5-μm-thick films spun-cast onto ITO/glass substrates. After drying overnight in a vacuum oven at room temperature, 200-nm-thick gold electrodes were thermally evaporated onto the top surface of the film. This sample preparation allows contact poling of the films and immediate ellipsometer measurements[18] to

(18) Khanarian, G.; Sounik, J.; Allen, D.; Shu, S. F.; Walton, C.; Goldberg, H.; Stamatoff, J. B. *J. Opt. Soc. Am. B* **1996**, *13*, 1927.

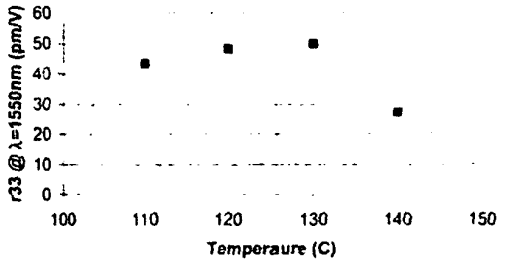

Figure 8. r_{33} dependence on poling temperature for a constant poling field of 100 V/μm for compound **4**.

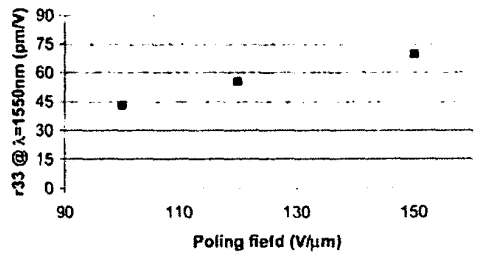

Figure 9. r_{33} dependence on poling field for a constant poling temperature of 130 °C.

determine the electro-optic coefficient. Measurements of r_{33} were performed at both 1550- and 1300-nm wavelengths.

Determining the optimum poling conditions consisted of two steps. First, films were contact-poled for 30 min at 100 V/μm but at varying temperatures. Figure 8 shows the measured r_{33} values as a function of temperature.

Optimum poling occurred at 130 °C for 35% of **4** in polycarbonate. Next, the films were poled at the optimum temperature found by the proceeding experiment but with successively higher field strengths until dielectric breakdown of the film occurred. Figure 9 shows the maximum r_{33} (λ = 1550 nm) value of 70 pm/V was obtained for compound **4** by poling at 150 V/μm and 130 °C. We typically poled samples under 200 V/μm because some samples break down at that level. This value is twice the value of $LiNbO_3$. The r_{33} values measured at 1300 nm were on the average 14% higher than the measured values at 1550 nm. This is close to the 22% increase predicted by the wavelength dispersion of β. The difference is likely due to measurement error. To our knowledge, this is the best r_{33} value reported at 1550 nm to date. We believe that there are mainly two reasons that contribute to this result. First, our unique acceptor design allows us to have very differently sized R_1 and R_2 groups. This size difference generates a chromophore with a fishhook shape that creates a great increase in chromophore solubility, resulting in an increased doping concentration. Second, the three-dimensional fishhook structure helps to keep chromophore–chromophore electrostatic interactions to a low level, resulting in more efficient poling.

Conclusion

We have successfully synthesized four new high $\mu\beta$ chromophores. These chromophores possess isophorone and combined isophorone–dialkylthiophene bridges. All chromophores take advantage of our newly synthesized

novel acceptors, rendering them very soluble in nonpolar solvents and polycarbonates. Since these acceptors have unique furan ring structures including spiro ring junctions, by selection of R_1 and R_2 groups of different sizes, electronic properties, and flexibility, all our newly synthesized chromophores have good solubility and high processibility. UV spectra show all the chromophores exhibit large solvatochromic effects, implying these new chromophores possess very large $\mu\beta$ values. Preliminary EO characterization demonstrates that chromophore **4** has an extremely high EO activity with a value of 70 pm/V r_{33} being achieved at 1550 nm as measured by elipsometry. Thermal testing indicates the chromophores are very stable with the majority of them stable to over 250 °C in air. Good thermal stability allows us more choices of how to process these chromophores into different polymer matrixes. We are continuing to characterize these chromophores and are actively working on obtaining pure enantiomers from the racemate. We will continue to report our results as they become available.

Experimental Section

General Information. ^{1}H NMR, ^{13}C NMR, and ^{19}F NMR were obtained with a Varian Unity Inova 300-MHz system. TMS was used as the internal standard. $CDCl_3$ was used as solvent unless specified otherwise. Gas chromatography/mass spectrometry (GC/MS) data were obtained using a Varian Saturn 200 system. Matrix-assisted laser desorption ionization Fourier transform ion cyclotron resonance mass spectrometry (MALDI−FTICR/MS) was performed on an IonSpec Ultima II (IonSpec Corp., Irvine, CA) 7T Fourier transform mass spectrometer. The neat samples, dissolved in methylene chloride, were mixed with a 0.5 M solution of 2,5-dihydroxybenzoic acid and allowed to co-crystallize. External calibration with a standard of poly(ethylene glycol) (M_w = 1000) was provided. The theoretical exact mass for all the compounds was obtained as the protonated adduct, the sodium adduct, the carbon 13 satellite of the sodium adduct, and the theoretical exact mass for the radical cation formed by loss of an electron. The observed mass for the cation adduct, the observed mass for the protonated adduct, the observed mass for the sodium adduct, and the observed mass for the carbon 13 satellite of the sodium adduct and the deviation between these two mass values in Daltons and in parts per million are reported. All deviations were found to be less than 10 ppm for all cases. In this paper, the exact mass of protonated adduct will be given. Additional results have been supplied in the Supporting Information. Melting points were obtained from A Mel-Temp 3.0 device and are uncorrected. UV−Vis−NIR spectra were obtained using a Perkin-Elmer Lambda 900 spectrometer. TGA were performed using a Seiko TG/DTA 220. The conditions were as follows: atmosphere, air at 100 mL/min; heat cycle, 20−400 °C at 10 °C/min; sample size of 2.5−3.5 mg; 5% weight loss was taken as the onset of decomposition to avoid any residual solvent in the sample leading to error in the data.

3-(*p*-*N*,*N*-Diethylaminostyryl)-5,5-dimethylcyclohex-2-enone (1). 4-Diethylaminobenzaldehyde (17.7 g, 0.10 mol), isophorone (13.8 g, 0.10 mol), NaOH (8.0 g, 0.20 mol), ethanol (100 mL), and water (50 mL) were mixed at room temperature. The mixture was stirred at room temperature for 96 h. Solid formed in the reaction solution after 3 days of stirring. After filtering the solid from the reaction mixture, the solid was redissolved into ethyl acetate (300 mL) and washed with brine (100 mL) and water (2 × 50 mL) and dried over anhydrous $MgSO_4$. After the solvent was evaporated, the solid was slurred by adding ether to the flask. The solid was then collected by vacuum filtration to yield 17.8 g, 59.9%. mp 95.2−97.0 °C. ^{1}H NMR: δ 8.04 (d, 1H), 7.54 (d, 2H), 7.55−7.479 (m, 1H), 7.38 (m, 1H), 6.76 (d, 2H), 3.42 (q, 4H), 2.87 (s, 2H), 2.49 (s, 2H), 1.20 (t, 6H), 1.09 (s, 6H). Molecular formula: $C_{20}H_{27}NO$. Exact mass + H: calculated, 298.2171; observed, 298.2172.

Tributyl(1,3-dioxolan-2-ylmethyl)phosphonium Bromide (2). Compound **2** was made following the method from ref 19. 1,3-Dioxolan-2-ylmethyl bromide was reacted with tributylphosphine quantitatively at 90 °C to yield the salt as a glass without needing further purification. ^{1}H NMR: δ 5.28 (t, 1H), 4.10 (m, 4H), 3.13 (d, 2H), 2.50 (m, 6H), 1.48 (m, 12H), 0.94 (t, 9H).

3-{3-(*p*-*N*,*N*-Diethylaminostyryl)-5,5-dimethylcyclohex-2-enylidene}-2-butenal (3). *Method A*: To a solution of compound **1** (12.0 g, 0.041 mol) and compound **21** (0.048 mol) in THF (200 mL), potassium *tert*-butoxide (60 mL, 0.06 mol, 1 M in THF) was added dropwise. The mixture was refluxed overnight and the solvent was then removed. The organic material was extracted with ethyl ether (3 × 100 mL) from its water mixture. The combined organic extracts were washed with brine (2 × 100 mL) and water (100 mL) and dried over anhydrous $MgSO_4$. Aldehyde **3** was obtained as cis−trans isomers from a silica gel chromatograph column (10% ethyl acetate in hexane) to yield 5.3 g, 40.0%.

Method B: A solution of butyllithium (16.2 mL, 0.041 mol, 2.5 M in hexane) was added dropwise to a solution of diisopropylamine (4.08 g, 0.041 mol) in dry ether at 0 °C. This fresh LDA solution was stirred for 10 min at 0 °C and cooled to −78 °C. *N*-Cyclohexylacetaldimine (5.06 g, 0.041 mol) was added dropwise to the above LDA solution. The mixture was then slowly warmed to −10 °C and cooled back to −78 °C. Compound **1** (10.0 g, 0.034 mol) dissolved in 30 mL of ethyl ether was added dropwise to the Vilsmeier reagent. This final mixture was allowed to slowly warm to room temperature, stirred overnight, at room temperature, and poured into water (100 mL). The organic product was extracted with ethyl ether (2 × 100 mL). The combined organic layers were washed with brine (2 × 100 mL) and water (2 × 50 mL) and dried over anhydrous $MgSO_4$. After removal of the solvent, the cis−trans isomers of **3** were obtained from a silica gel chromatography column (10% ethyl acetate in hexane) to yield 5.7 g of **3**, 52.4%. The aldehyde proton peak at 10.23 is the cis isomer and the proton peak at 10.06 is the trans isomer. The NMR estimate of cis/trans is 34:64%. This result was obtained for both methods. Mixed isomers mp 88.0−91.0 °C. Trans isomer ^{1}H NMR: δ 10.06 (d, 1H), 7.35 (d, 2H), 6.76 (s, 2H), 6.05 (d, 2H), 6.26 (s, 1H), 5.92 (dd, 1H), 3.40 (q, 4H), 2.68 (d, 2H), 2.35 (s, 2H), 1.22 (t, 6H), 1.06 (s, 6H). Molecular formula: $C_{22}H_{29}NO$. Exact mass + H: calculated, 324.2327; observed, 324.2330.

2-{[3-[2[4-(Diethylamino)phenyl]ethenyl]-5,5-dimethyl-2-cyclohexen-1-ylidene]methyl}thiophene (9). Sodium ethoxide (50 mL, 0.05 mol, 1 M in ethanol) was added dropwise to a mixture of compound **1** (10.0 g, 0.034 mol) and **8** (22.3 g, 0.041 mol) in DMF (50 mL). The mixture was heated to 100 °C and stirred for 48 h before being poured into water (200 mL). The organic mixture was extracted with ethyl ether (3 × 100 mL). The combined organic layers were washed with brine (2 × 50 mL) and water (2 × 50 mL) and dried over anhydrous $MgSO_4$. Pure compound **9** was obtained from a silica gel chromatography column (5% ethyl acetate in hexane) to yield 11.0 g, 59.8%. ^{1}H NMR: δ 7.32 (d, 2H), 6.85 (s, 1H), 6.76−6.48 (m, 3H), 6.65 (d, 2H), 6.29 (s, 1H), 3.76 (q, 4H), 2.52 (m, 6H), 2.23 (s, 2H), 1.65−1.27 (m, 16H), 1.19 (t, 6H), 1.03 (s, 6H), 0.90 (m, 6H). Molecular formula: $C_{37}H_{55}NS$. Exact mass + H: calculated, 546.4133; observed, 546.4156.

2-{[3-[2[4-(Diethylamino)phenyl]ethenyl]-5,5-dimethyl-2-cyclohexen-1-ylidene]3-propylidene}thiophene (10). Compound **10** was made according to the method outlined for compound **9**. Compound **3** (1.43 g, 0.0044 mol), **9e** (2.9 g, 0.0053 mol), and sodium ethoxide (7.0 mL, 0.007 mol) yielded compound **10** (1.8 g, 71.6%). ^{1}H NMR: δ 7.31 (d, 2H), 6.71 (s, 1H), 6.91 (m, 1H), 6.70−6.61 (m, 3H), 6.52−6.44 (m, 1H), 6.64 (d, 2H), 6.19 (s, 1H), 3.37 (q, 4H), 2.56 (t, 2H), 2.47 (t, 2H), 2.31

(19) Spangler, C. W.; Liu, P.-K.; Dembek, A. A.; Havelka, K. O. *J. Chem. Soc., Perkin Trans.* **1991**, *1*, 799.

varied from 3×10^{12} to 1×10^{15} photons cm^{-2} at 430 nm, using a bank of auto-insertable neutral density filters. For all of the experiments reported, the light was incident on the TiO_2 side of the bilayer. The photo-induced conductivity of the sample was measured by the change in the microwave power reflected by the cavity at resonance, using the time-resolved microwave conductivity technique (TRMC) [15,22]. The overall response-time of detection of 18 ns was determined mainly by the loaded quality factor of the cavity. The integrated laser pulse convoluted with the response time is shown as the dashed line in Figure 1.

Received: April 10, 2002
Final version: August 13, 2002

[1] M. Grätzel, *Nature* **2001**, *414*, 338.
[2] B. O'Regan, M. Grätzel, *Nature* **1991**, *353*, 737.
[3] P. V. Kamat, *Chem. Rev.* **1993**, *93*, 267.
[4] A. Hagfeldt, M. Grätzel, *Chem. Rev.* **1995**, *95*, 49.
[5] A. Hagfeldt, M. Grätzel, *Acc. Chem. Res.* **2000**, *33*, 269.
[6] A. Kay, R. Humphrybaker, M. Grätzel, *J. Phys. Chem.* **1994**, *98*, 952.
[7] D. Liu, P. V. Kamat, *J. Chem. Phys.* **1996**, *105*, 965.
[8] S. Barazzouk, H. Lee, S. Hotchandani, P. V. Kamat, *J. Phys. Chem. B* **2000**, *104*, 3616.
[9] K. Kalyanasundaram, N. Vlachopoulos, V. Krishnan, A. Monnier, M. Grätzel, *J. Phys. Chem.* **1987**, *91*, 2342.
[10] J. Kallioinen, G. Benko, V. Sundstrom, J. E. I. Korppi-Tommola, A. P. Yartsev, *J. Phys. Chem. B* **2002**, *106*, 4396.
[11] J. E. Kroeze, T. J. Savenije, J. M. Warman, *J. Photochem. Photobiol., A* **2002**, *148*, 49.
[12] Y. Tachibana, S. A. Haque, I. P. Mercer, J. R. Durrant, D. R. Klug, *J. Phys. Chem. B* **2000**, *104*, 1198.
[13] R. W. Fessenden, P. V. Kamat, *J. Phys. Chem.* **1995**, *99*, 12 902.
[14] T. J. Savenije, M. J. W. Vermeulen, M. P. De Haas, J. M. Warman, *Sol. Energy Mater. Sol. Cells* **2000**, *61*, 9.
[15] T. J. Savenije, M. P. De Haas, J. M. Warman, *Z. Phys. Chem. (Leipzig)* **1999**, *212*, 201.
[16] N. J. Turro, *Modern Molecular Photochemistry*, The Benjamin/Cummings Publishing Co., Inc., Menlo Park, CA **1978**.
[17] J. Singh, *Excitation Energy Transfer Processes in Condensed Matter*, Plenum, New York **1994**.
[18] S. P. McGlynn, T. Azumi, M. Kinoshita, *Molecular Spectroscopy of the Triplet State*, Prentice Hall, Englewood Cliffs, NJ **1969**.
[19] A. Harriman, *J. Chem. Soc. Faraday Trans. 1* **1980**, *76*, 1978.
[20] A. Harriman, *J. Chem. Soc. Faraday Trans. 2* **1981**, *77*, 1281.
[21] R. van de Krol, A. Goossens, J. Schoonman, *J. Phys. Chem. B* **1999**, *103*, 7151.
[22] M. P. De Haas, J. M. Warman, *Chem. Phys.* **1982**, *73*, 35.
[23] K. Kalyanasundaram, M. Neumann-Spallart, *J. Phys. Chem.* **1982**, *86*, 5163.
[24] F. J. Vergeldt, R. B. M. Koehorst, T. J. Schaafsma, J.-C. Lambry, J.-L. Martin, D. G. Johnson, M. R. Wasielewski, *Chem. Phys. Lett.* **1991**, *182*, 107.

Design, Synthesis, and Properties of Highly Efficient Side-Chain Dendronized Nonlinear Optical Polymers for Electro-Optics**

By *Jingdong Luo, Sen Liu, Marnie Haller, Lu Liu, Hong Ma,* and *Alex K-Y. Jen**

Organic polymeric second-order nonlinear optical (NLO) materials have attracted considerable attention due to their potential applications in ultrahigh-speed electro-optic (EO) switches and modulators.[1,2] One major obstacle that hinders the rapid development of this technology is the lack of an effective mechanism to translate high-molecular nonlinearities ($\mu\beta$) into large macroscopic EO activities (r_{33}). In general, the strong intermolecular electrostatic interactions among high-dipole-moment NLO chromophores significantly decrease the poling efficiency of these materials.[3] Recently, the concept of using shape modification of NLO chromophores to improve poling efficiency has been demonstrated by Dalton et al. to somewhat alleviate this problem.[3,4] By applying a similar site-isolation principle to EO polymers, we have developed a NLO dendrimer with a crosslinkable periphery, exhibiting a large r_{33} value and excellent thermal stability.[5] Since the globular geometry of dendrimers is suited for the modification of chromophores to the ideal spherical shape, this encouraging result demonstrates that dendritic structure can be employed as a very promising molecular topology for the next generation of highly efficient EO materials.[6]

More recently, a NLO chromophore encapsulated by highly fluorinated dendrons has been synthesized.[7] When comparing this chromophore to its pristine analog, this 3D shaped dendritic chromophore displays a significant blue-shifted absorption (~40 nm), lower optical loss, and an almost three times higher EO response. Conspicuously, all these desirable materials properties can be simultaneously achieved in an amorphous polycarbonate. This indicates that the site-isolation effect can also work very well at the local domains of the encapsulated chromophores within a linear polymer matrix. The synthesis of chromophore-containing EO dendrimers, especially those with high molecular weights and reasonable film-forming properties, requires lengthy and tedious synthetic steps. In order to shorten the time needed for developing highly efficient EO materials, we have applied the site-isolation principle to some linear polymer systems to convert them into dendron-substituted polymers, i.e., dendronized polymers.

Dendronized polymers are a new class of linear polymers bearing pendant dendrons on the repeated units, and the development of dendronized polymers over the last decade has demonstrated their great potential for applications in many areas, ranging from materials science to biosciences.[8,9] Controlled by the size, shape, and density of the attached dendritic side chain moieties, and the degree of polymerization, the backbone of the polymers can be manipulated from a random-coil to an extended rigid rod. As a result, the dendronized-polymer conformation will shift from spherical to cylindrical.[8] This provides the possibility of achieving unique and nanoscale tuning in polymer properties. To take advantage of the unique conformational changes in dendronized polymers for developing highly efficient EO materials, we have incorporated the trifluorovinylether-containing dendritic moieties into the chromophore-grafted polymers, to obtain two NLO dendronized polymers. Functionalizing bulky dendritic moieties onto both the side chain chromophores, and the polystyrene backbone, allows us to achieve a psuedo-cylindrical polymer conformation. As a result, the strong chromophore–

[*] Prof. A. K.-Y. Jen, Dr. J. Luo, S. Liu, M. Haller, Dr. L. Liu, Dr. H. Ma
Department of Materials Science and Engineering, Box 352120
University of Washington, Seattle, WA 98195-2120 (USA)
E-mail: ajen@u.washington.edu

[**] Financial support from the National Science Foundation (NSF-NIRT) and the Air Force office of Scientific Research (AFOSR) are acknowledged. A. K-Y. Jen thanks the Boeing-Johnson Foundation for its support.

  0935-9648/02/2312-1763 $ 17.50+.50/0

chromophore electrostatic interactions, and the polymer interchain entanglement can be suppressed. Here, we report the synthesis and characterization of two side-chain NLO dendronized polymers that exhibit exceptionally high r_{33} values.

Although several elegant synthetic approaches exist that can produce dendronized polymers through the polymerization of "macromonomers", which are monomers functionalized with a dendron,[10] most of the highly polarizable NLO chromophores cannot survive these polymerization conditions due to their chemical sensitivity. Thus, it is desirable to utilize the post-functionalization approach.[11] This allows chromophores to be introduced into reactive precursor polymers at the final stage, without exposing them to vigorous polymerization conditions.

In this regard, we have developed a novel synthetic route to attach highly active chromophores onto the polymer backbone as side chains (Schemes 1 and 2). This method, unlike most of the reported ones,[11] can be applied to compounds **1a** and **1b**, two of the most efficient chromophores, to obtain very good yields. The acceptor end of **1a** and **1b** is first capped with a dendron, via the esterification reaction between their hydroxyl groups and the carboxylic acid group of **2**.[12] The methoxymethyl (MOM) groups of the intermediates were then cleaved by bromotrimethylsilane, and the newly formed hydroxyl groups were converted into the semi-ester derivatives **5a** and **5b** of phthalic acid.[13,14]

By using 1,3-dicyclohexylcarbodiimide (DCC) and 4-(dimethylamino)-pyridinium 4-toluenesulfonate (DPTS) as the condensation reagents, poly(4-vinylphenol) **6**, a polymer purchased from Aldrich with a weight-averaged molecular weight (M_w) of ~20000, was condensed sequentially with the dendron-capped **5a** and **5b**, and a smaller trifluorovinylether-containing acid **7**, to afford the side-chain NLO dendronized polymers **8a** and **8b**, respectively. These two steps proceeded in one pot under very mild conditions. The introduction, distribution, and relative composition of different side-chain moieties can be tuned by changing the loading procedures. The resulting by-products,[12] such as the *N*-acylurea and anhydride intermediates, can be removed by repetitive precipitation.

Both of the chromophore loading levels in polymer **8a** and **8b** were maintained at about 20 wt.-%. This was confirmed by the relative integration comparison of the corresponding characteristic peak in their NMR spectra, and the quantitative analysis of the UV-vis spectra of their solutions in 1,4-dioxane. The molecular weight and structures of these dendronized polymers were fully characterized by gel permeation chromatography, ^{1}H and ^{19}F NMR spectroscopy, and elemental analysis. With the identical loading molar ratio of the two different

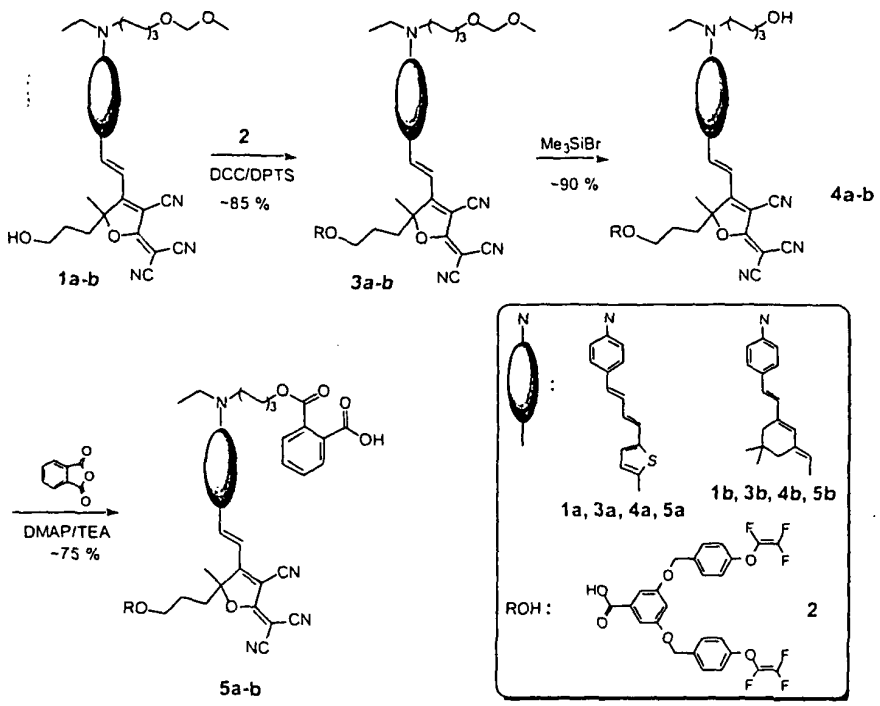

Scheme 1. Synthesis of dendron-attached, and phthaloylated chromophore derivatives. DCC: 1,3-dicyclohexylcarbodiimide; DPTS: 4-(dimethylamino)-pyridinium 4-toluenesulfonate; TEA: triethylamine; DMAP: 4-(dimethylamino)pyridine.

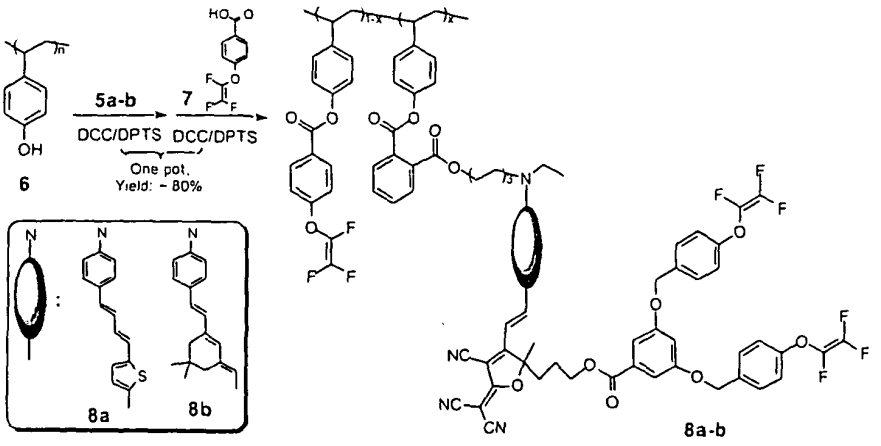

Scheme 2. Synthesis of side-chain dendronized NLO polymers by one-pot postesterification.

  0935-9648/02/2312-1764 $ 17.50+.50/0 *Adv. Mater.* 2002, *14*, No. 23, December 3

side groups, the polymer **8a** has a M_w of 88410 and a polydispersity (PD) of 2.24, very close to those of 86620 and 2.22 for **8b**, indicating good reproducibility in these post-functionalization reactions. The combined advantages of simple procedures and very mild synthetic conditions make this methodology widely applicable for making NLO side-chain polymers and other functional materials.

These dendronized polymers also possess good solubility in common organic solvents, such as methylene dichloride, tetrahydrofuran (THF), and cyclopentanone. The high molecular weights give the polymers excellent film-forming ability. The UV-vis spectra of **8a** and **8b** in 1,4-dioxane exhibit strong absorption maxima at 648 nm and 661 nm, respectively ascribed to the π–π^* charge-transfer bands of the NLO chromophores. Thermal analysis by differential scanning calorimetry shows typical glass transition behavior around 90 °C for **8a** and 95 °C for **8b**. At temperatures above ~150 °C, both of them display similar exothermic peaks, corresponding to the crosslinking reaction of the trifluorovinylether groups.[15]

For EO measurements, the solution of **8a** in cyclopentanone (13 wt.-%, filtered through a 0.2 μm syringe filter) was spin-coated onto indium tin oxide (ITO) glass substrates. The films were baked under vacuum at 85 °C overnight to ensure removal of the residual solvent. A thin layer of gold was then sputtered onto the films as the top electrode for performing the high-electric-field poling. The films were poled at 95 °C with a DC electric field of 1.42 MV cm^{-1}. The r_{33} value was measured using the reflection technique at 1.3 μm,[16] and the poled films of **8a** showed a very large EO coefficient (r_{33} = 81 pm V^{-1}).

For the purpose of comparison, EO properties of several conventional polymeric systems bearing similar chromophores were also studied. Among them, chromophores **9** and **10** (Fig. 1), without and with the shape-modification side group, respectively, were formulated into a polymer matrix poly(methylmethacrylate) (PMMA) (**9** and **10**) or amorphous polycarbonate (APC) (**9** only) to afford three guest–host systems. Polymer **14**, which is a typical side-chain NLO polymer without any dendritic moieties, has also been synthesized according to the procedure in Scheme 3 for direct comparison. The only difference between this route and the route depicted in Scheme 1 and 2, is that dimethylformamide (DMF) was added as the co-solvent in the postesterification reaction to improve the solubility of **13** in the reaction mixtures. In Scheme 1 this was unnecessary, since chromophores **5a** and **5b**, with the same polar carboxylic acid groups, are highly soluble in common organic solvents such as methylene dichloride, THF, and acetone. Apparently, the dendritic encapsulation significantly reduces the tendency of chromophore crystallization that is usually driven by strong intermolecular electrostatic interactions. The chromophore loading density for all these materials was normalized at the level of 20 wt.-%, the same as that for **8a**, and the r_{33} values listed in Table 1 are the highest achievable ones after optimizing the poling conditions. For example, the films of **14** were poled at 125 °C, a temperature around its glass transition temperature, with the same high DC electric field of 1.42 MV cm^{-1} as that for **8a**.

The EO activity of the side-chain dendronized polymer **8a** is significantly higher than those of the guest–host systems and the pristine side-chain polymer **14**. The lower EO coefficients of the poled films of **9** in PMMA, **9** in APC, **10** in PMMA, and **14**, indicate that the strong chromophore–chromophore electrostatic interactions severely limit the attainable EO activities in ordinary NLO polymers without the effective site isolation. Although other factors, such as conductivity of the samples and chain flexibility of different matrix polymers, may also affect the achievable EO activities in materials, these are limited to a minor contribution since both of the side-chain polymers **8a** and **14** possess the same polystyrene-based backbone. In addition, the same electric field has been applied to pole these films. Nevertheless, the r_{33} value of side-chain NLO dendronized polymer **8a** is two-and-a-half times higher than that of the pristine side-chain NLO polymer **14**. Therefore, the high poling efficiency in the poled films **8a**, to a large extent, is due to the site-isolation effect that allows the chromophore to be spatially well distributed and efficiently orientated. This is also quite consistent with the poling behaviors obtained from the EO dendrimer and the dendritic NLO chromophore that we previously reported.[15,6]

In terms of alignment stability, these side-chain dendronized polymers also exhibit very promising results: the poled polymer **8a** without crosslinking, and even with such large side groups, retains higher than 90 % of its original r_{33} value after several hundred hours at room temperature. This may be due to the steric hindrance caused by the large dendrons that inhibits the free rotation of the polymer chains.

By applying this new molecular engineering approach to a CLD-type chromophore (a more efficient NLO molecule), an extremely large EO coefficient (r_{33} = 97 pm V^{-1} at 1.3 μm) has been achieved for the poled side-chain NLO dendronized polymer **8b**. To our knowledge, this value is the highest one ever reported for the side-chain NLO polymers. This value is also superior to those of the reported values for CLD-based guest–host EO polymer systems (Fig. 2 and Table 2).

For those CLD-based guest–host material systems, the r_{33} values listed in Table 2 are the highest achievable ones after optimizing the loading density chromophores.

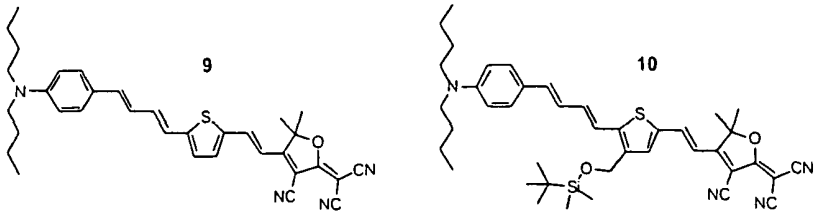

Fig. 1. Chromophores **9** and **10** of guest–host systems for comparison.

0935-9648/02/2312-1765 $ 17.50+.50/0

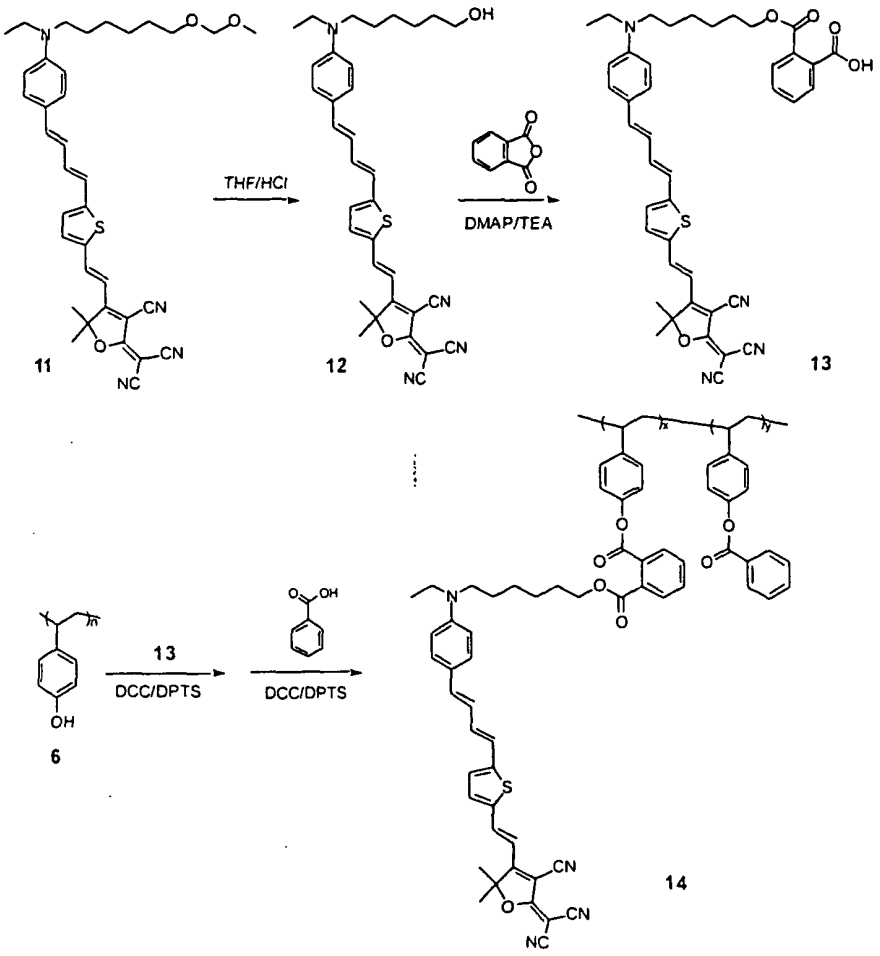

Scheme 3. Synthesis of side-chain NLO polymer **14** by one-pot postesterification.

Table 1. Comparison of electro-optic activities between side-chain dendronized NLO polymer **8a** and conventional guest-host or side-chain polymeric systems with the similar chromophores.

Material systems	Electro-optic coefficient (r_{33}) [pm V^{-1}] at 1.3 μm
dendronized polymer (**8a**)	81
chromophore **9**/PMMA	45
chromophore **9**/APC	34
chromophore **10**/PMMA	49
side-chain polymer **14**	33

Compared with them, the dendronized polymer **8b** exhibits a 50 % higher EO coefficient even with a 50 wt.-% lower chromophore loading density. Furthermore, polymer **8b** displays the similar alignment stability as that of polymer **8a**.

Although EO activities for highly efficient chromophores such as the CLD-type chromophore is usually compromised to a certain extent by the strong intermolecular electrostatic interactions, this exceptionally high experimental r_{33} value of 97 pm V^{-1} agrees fairly well with the highest achievable value of 124 pm V^{-1} predicted by theory using a two-level model suggested by Singer et al.[17] By accounting for the dispersion effects from both the electric-field-induced second harmonic generation (EFISH) and electro-optic measurements, the r_{33} is expressed as

$$r_{33} = (4/n^4)N(f_\omega)^2(f_0)^2(\beta_z\mu/5kT)E_pF_1(\omega_0,\omega')/F_2(\omega_0,\omega) \quad (1a)$$

where N is the number density of the chromophores, n is the index of fraction, f_0 and f_ω are the local field factors

$$f_0 = \varepsilon(n^2+2)/(n^2+2\varepsilon) \quad (1b)$$

and

$$f_\omega = (n^2+2)/3 \quad (1c)$$

and F_1 and F_2 are the dispersion factors

$$F_1(\omega_0,\omega') = \omega_0^4/[(\omega_0^2-\omega'^2)(\omega_0^2-4\omega'^2)] \quad (1d)$$

and

$$F_2(\omega_0,\omega) = \omega_0^2(3\omega_0^2-\omega^2)/[3(\omega_0^2-\omega^2)^2] \quad (1e)$$

  0935-9648/02/2312-1766 $ 17.50+.50/0 *Adv. Mater.* 2002, *14*, No. 23, December 3

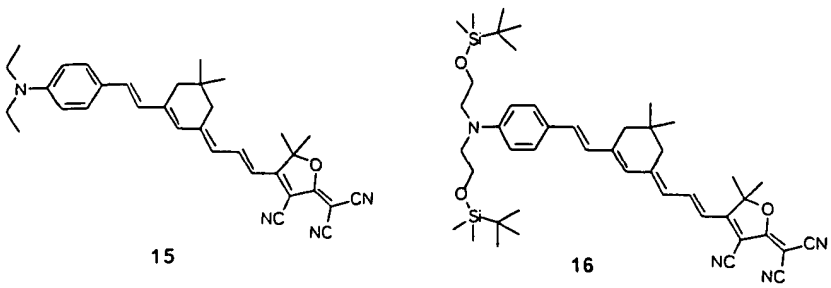

Fig. 2. Chromophores **15** and **16** used in the guest–host systems for comparison.

Table 2. Comparison between CLD-based guest–host systems and side-chain dendronized NLO polymer **8b**.

Material systems	Loading density of chromophores [wt.-%]	Electro-optic coefficient (r_{33}) [pm V^{-1}] at:	
		1.06 μm	1.3 μm
8b	20	N. A.	97
16/APC	30	90	~65
16/PMMA	30	85	~60

Here ω' is the optical frequency used in the EFISH measurement, ω is the frequency adopted in the electro-optic measurement, and ω_0 is the transition energy between the ground state and first excited state of the chromophore. Therefore, ~80 % of the theoretically achievable EO activity deriving from the highly efficient CLD-type chromophore has been accomplished in the poled polymer **8b**. This further verifies that the side-chain dendronized polymer is a very promising molecular design for enhancing EO property of the polymers.

In conclusion, we have developed a simple and generally applicable method for the post-functionalization of side-chain dendronized NLO polymers. This approach provides the combined advantages of achieving better poling efficiency through the site-isolation effect and shortening the time required for EO dendrimer synthesis. High poling efficiency has been achieved to afford an exceptionally large EO coefficient (97 pm V^{-1} at 1.3 μm). A comprehensive study of how to enhance the poling-induced alignment stability at higher temperatures through crosslinking of the peripheral trifluorovinyl ether groups is in progress.

Experimental

Methylene dichloride was distilled over phosphorus pentoxide under nitrogen. Tetrahydrofuran (THF) was distilled from sodium benzophenone ketyl under nitrogen prior to use. 4-(Dimethylamino)-pyridinium 4-toluenesulfonate (DPTS) was prepared according to the literature [12]. The synthesis of compounds **1a**, **1b**, **2**, and **11** will be reported elsewhere. All the other chemicals were purchased from Aldrich unless otherwise specified.

Preparation of Compound 3a: The mixture of compound **1a** (0.67 g, 1.03 mmol), **2** (0.7 g, 1.32 mmol), and DPTS (0.08 g, 0.27 mmol) was stirred in methylene dichloride for 15 min. 1,3-Dicyclohexylcarbodiimide (DCC) (0.33 g, 1.60 mmol) was added, and the reaction mixture was stirred at room temperature overnight. After filtration, all the solvent was evaporated under reduced pressure. The crude product was purified by column chromatography using ethyl acetate/hexane (3:2, by volume) as the eluent to afford **3a** as blue–greenish oil (0.91 g, 76 %). R_f = 0.65 (silica gel, 3:2 ethyl acetate/hexane).

Preparation of Compound 4a: To a cooled solution of compound **3a** (0.90 g, 0.78 mmol) in methylene dichloride, under the protection of nitrogen, 2.5 mL (18.9 mmol) of bromotrimethylsilane was added dropwise. The reaction mixture was stirred at −30 °C for 2.5 h, and then neutralized with 50 mL of saturated aqueous solution of sodium bicarbonate. The residue was partitioned between the water and CH_2Cl_2, and the aqueous layer was extracted with CH_2Cl_2. The combined extracts were dried over sodium sulfate. The crude product was purified by flash chromatography to obtain **4a** as a blue–greenish solid (0.4 g, 87 %) and retrieve 0.42 g of **3a**. R_f = 0.48 (silica gel, 2:1 ethyl acetate/hexane). ^{1}H NMR ($CDCl_3$, TMS, ppm): δ 7.70 (d, J = 15.6 Hz, 1H), 7.42 (d, J = 8.3 Hz, 4H), 7.31 (d, J = 8.8 Hz, 2H), 7.16–7.28 (m, 4H), 7.12 (d, J = 8.3 Hz, 4H), 6.87–7.02 (m, 1H), 6.84 (d, J = 4.2 Hz, 1H), 6.66–6.80 (m, 3H), 6.20 (d, J = 8.7 Hz, 2H), 6.53 (d, J = 15.6 Hz, 1H), 5.01 (s, 4H), 4.33 (t, J = 6.7 Hz, 2H), 3.66 (t, J = 6.7 Hz, 2H), 3.41 (q, J = 6.8 Hz, 2H), 3.30 (t, J = 7.8 Hz, 2H), 2.18–2.37 (m, 1H), 1.99–2.15 (m, 1H), 1.74 (s, 3H), 1.23–1.68 (m), 1.18 (t, J = 7.2 Hz, 3H).

Preparation of Compound 5a: To a solution of compound **4a** (0.19 g, 0.17 mmol), triethylamine (0.10 mL), and 4-(dimethylamino)pyridine (DMAP, 0.010 g, 0.082 mmol) in 5 mL of CH_2Cl_2, was added 0.031 g of phthalic anhydride (0.21 mmol). After stirring overnight at room temperature, the solution was sequentially washed with 1 N HCl solution, dilute sodium bicarbonate solution and water, and dried over sodium sulfate. The crude product was purified by flash column chromatography with a gradient eluent of CH_2Cl_2/acetone (6:1, by volume) to CH_2Cl_2/acetone (3:1, by volume) to afford **5a** as a blue–greenish solid (0.13 g, 60 %). R_f = 0.34 (silica gel, 2:1 ethyl acetate/hexane). ^{1}H NMR (DMSO-d_6, ppm): δ 8.06 (d, J = 15.6 Hz), 7.68–7.77 (m, 1H), 7.55–7.65 (m, 3H), 7.50 (d, J = 8.3 Hz, 4H), 7.19–7.36 (m, 6H), 6.97–7.14 (m, 4H), 6.55–6.93 (m, 8H), 5.09 (s, 4H), 4.04–4.40 (m, 4H), 2.17–2.57 (m), 1.78 (s, 3H), 1.17–1.73 (br m, 12H), 1.06 (t, J = 6.7 Hz, 3H).

Preparation of Side-Chain Dendronized NLO Polymer 8a: To a solution of **5a** (0.125 g, 0.099 mmol), poly(4-vinylphenol) (0.054 g, 0.45 mmol), and DPTS (0.012 g, 0.04 mmol) in a mixture of 6 mL of THF and 3 mL of CH_2Cl_2 was added 0.025 g of DCC (0.121 mmol). The reaction mixture was allowed to stir at room temperature for 12 h under nitrogen. 0.094 g of compound **7** (0.43 mmol), 0.031 g of DPTS (0.11 mmol), and 0.106 g of DCC (0.51 mmol) were then added, and stirred at room temperature for 40 h. Iterative dissolution and filtration removed most of the resultant urea. The filtered CH_2Cl_2 solution was then added dropwise to the stirring methanol. The precipitate was collected, and reprecipitation by adding dropwise its CH_2Cl_2 solution into methanol afforded polymer **8a** as a blue–greenish solid (0.207 g, yield ~80 %). ^{1}H NMR ($CDCl_3$, TMS, ppm): δ 8.03 (br s), 7.57–7.86 (br m), 7.41 (d, J = 8.3 Hz), 6.31–7.32 (br m), 4.995 (s), 3.98–4.49 (br m), 2.96–3.47 (br m), 0.56–2.41 (br m). ^{19}F NMR ($CDCl_3$, C_6F_6, ppm): −136.9 – −135.8 (br m), −135.35 (dd, J = 61 Hz), −127.8 (dd, J = 97.7 Hz), −127.2 (br s), −126.8 (br s), −126.4 (br s), −120.9 (dd, J = 61 Hz), −120.2 (br m), −120.0 (br s), −119.9 (br s), −119.7 (br s). A UV-vis spectrum in 1,4-dioxane showed λ_{max} = 648 nm. Molecular weight: M_w = 88 410 with a polydispersity of 2.24. T_g = 90 °C.

Compound **3b**, **4b**, **5b**, and polymer **8b** were prepared following the similar procedure of **3a**, **4a**, **5a**, and **8a**, respectively.

Compound 4b: The product was obtained as the mixture of trans and cis isomers. R_f = 0.27 (silica gel, 3:2 ethyl acetate/hexane). The *cis*-isomer peaks cannot be fully identified due to their weak intensity [19]. The arbitrary assignment of the ^{1}H NMR peaks ($CDCl_3$, TMS, ppm) of the *trans*-isomer, the majority part of the product, is: δ 7.99 (q, J_1 = 12.97 Hz, J_2 = 14.02 Hz, 1H), 7.43 (d, J = 8.3 Hz, 4H), 7.34 (d, J = 8.8 Hz, 2H), 7.19–7.29 (d, J = 2.1 Hz, 2H), 7.11 (d, J = 8.3 Hz, 4H), 6.84 (d, J = 16.08 Hz, 1H), 6.70–6.78 (m, 3H), 6.62 (d, J = 8.8 Hz, 2H), 6.25 (d, J = 12.4 Hz, 2H), 5.03 (s, 4H), 4.31 (t, 2H), 3.66 (t, J = 7.3 Hz, 2H), 3.22–3.47 (m, 4H), 2.13–2.44 (m, 5H), 1.87–2.09 (m, 1H), 1.68 (s, 3H), 1.24–1.66 (m, 10H), 1.19 (t, J = 6.2 Hz, 3H), 0.94–1.05 (d, J = 4.2 Hz, 6H).

Polymer 8b: ^{1}H NMR ($CDCl_3$, TMS, ppm): δ 8.00 (br s), 7.68 (br s), 7.41 (d, J = 8.3 Hz), 6.00–7.34 (br, m), 5.01 (s), 4.10–4.43 (br m), 3.08–3.46 (br m), 0.50–2.55 (br m). ^{19}F NMR ($CDCl_3$, C_6F_6, ppm): −136.8 – −135.7 (br m), −135.3 (dd, J = 54.9 Hz), −127.8 (dd, J = 97.7 Hz), −120.9 (dd, J_1 = 54.9 Hz, J_2 = 61.0 Hz), −120.2 (s), −120.1 – −119.5 (br m). A UV-vis spectrum in 1,4-dioxane showed λ_{max} = 661 nm. Molecular weight: M_w = 86 620 with a polydispersity of 2.22. T_g = 95 °C.

Preparation of Compound 12: To the solution of compound **11** (1.07 g, 1.75 mmol) in 25 mL of THF was added 20 mL of 6 N hydrochloride solution. The reaction mixture was allowed to reflux under nitrogen for 3 h. The cooled solution was neutralized by the aqueous solution of sodium bicarbonate. The solvent was then evaporated under reduced pressure. The residue was extracted by methylene dichloride and dried over sodium sulfate. The crude product was

  0935-9648/02/2312-1767 $ 17.50+.50/0

purified by flash column chromatography with CH_2Cl_2/ethyl acetate (4:1, by volume) to afford **12** as a blue-greenish solid (0.95 g, 96 %). R_f = 0.35 (silica gel, 4:1 CH_2Cl_2/ethyl acetate). ^{1}H NMR ($CDCl_3$, TMS, ppm): δ 7.74 (d, J = 15.6 Hz, 1H), 7.27–7.41 (m, 3H), 6.87–7.06 (m, 2H), 6.48–6.78 (m, 6H), 3.62 (t, 2H), 3.38 (q, 2H), 3.31 (t, 2H), 1.73 (s, 6H), 1.27–1.68 (m, 8H), 1.20 (t, 3H).

Preparation of Compound 13: Compound **13** was prepared following the same procedure as **5a** and **5b**. ^{1}H NMR (DMSO-d_6, ppm): δ 8.06 (d, 1H), 6.59–7.82 (br m, 15H), 4.15 (t, 2H), 1.80 (s, 6H), 1.25–1.65 (br m, 8H), 1.08 (t, 3H).

Preparation of Polymer 14: Polymer **14** was prepared following the same procedure as **8a** and **8b** except that the mixture of THF, CH_2Cl_2, and DMF was used as the reaction solvent (10:3:2 THF/CH_2Cl_2/DMF, by volume). ^{1}H NMR ($CDCl_3$, TMS, ppm): 7.92–8.37 (br s), 6.36–7.83 (br m), 4.21 (br s), 3.08–3.47 (br m), 0.60–2.42 (br m). A UV-vis spectrum in 1,4-dioxane showed λ_{max} = 645 nm. T_g = 125 °C.

Received: April 26, 2002
Final version: August 7, 2002

[1] a) *Molecular Nonlinear Optics: Materials, Physics and Devices* (Ed: J. Zyss), Academic Press, New York **1994**. b) S. R. Marder, B. Kippelen, A. K.-Y. Jen, N. Peyghambarian, *Nature* **1997**, *388*, 845.
[2] L. R. Dalton, W. H. Steier, B. H. Robinson, C. Zhang, A. Ren, S. Garner, A. Chen, T. Londergan, L. Irwin, B. Carlson, L. Fifield, G. Phelan, C. Kincaid, J. Amend, A. K-Y. Jen, *J. Mater. Chem.* **1999**, *9*, 19.
[3] a) L. R. Dalton, A. W. Harper, B. H. Robinson, *Proc. Natl. Acad. Sci. USA* **1997**, *94*, 4842. b) *L. R. Dalton, A. W Harper, Polym. News* **1998**, *23*, 114.
[4] a) B. H. Robinson, L. R. Dalton, *J. Phys. Chem. A*, **2000**, *104*, 4785. b) B. H. Robinson, L. R. Dalton, H. W. Harper, A. Ren, F. Wang, C. Zhang, G. Todorova, M. Lee, R. Aniszfeld, S. Garner, A. Chen, W. H. Steier, S. Houbrecht, A. Persoons, I. Ledoux, J. Zyss, A. K.-Y. Jen, *Chem. Phys.* **1999**, *245*, 35.
[5] H. Ma, B. Q. Chen, T. Sassa, L. R. Dalton, A. K.-Y. Jen, *J. Am. Chem. Soc.* **2001**, *123*, 986.
[6] a) H. Ma, A. K.-Y. Jen, *Adv. Mater.* **2001**, *13*, 1201. b) H. L. Bozec, T. L. Douder, O. Maury, A. Bondon, I. Ledoux, S. Deveau, J. Zyss, *Adv. Mater.* **2001**, *13*, 1677.
[7] J. Luo, H. Ma, M. Haller, A. K.-Y. Jen, R. R. Barto, *Chem. Commun.* **2002**, 888.
[8] a) L. Shu, A. D. Schlüter, C. Ecker, N. Severin, J. P. Rabe, *Angew. Chem. Int. Ed.* **2001**, *40*, 4666. b) V. Percec, C.-H. Ahn, G. Ungar, D. J. P. Yeardley, M. Möller, S. S. Sheiko, *Nature* **1998**, *391*, 161. c) A. D. Schlüter, *Top. Curr. Chem.* **1998**, *197*, 165. d) S. Hecht, J. M. J. Fréchet, *Angew. Chem. Int. Ed.* **2001**, *40*, 74. e) S. M. Grayson, J. M. J. Fréchet, *Chem. Rev.* **2001**, *101*, 3819. f) H. Frey, *Angew. Chem. Int. Ed.* **1998**, *37*, 2193.
[9] a) A. D. Schlüter, J. P. Rabe, *Angew. Chem. Int. Ed.* **2000**, *39*, 864. b) W. Stocker, B. L. Schürmann, J. P. Rabe, S. Förster, P. Lindner, I. Neubert, A. D. Schlüter, *Angew. Chem. Int. Ed.* **1998**, *10*, 793.
[10] a) V. Percec, C. H. Ahn, W. D. Cho, A. M. Jamieson, J. Kim, T. Leman, M. Schmidt, M. Gerle, M. Moeller, S. A. Prokhorova, S. S. Sheiko, S. Z. D. Cheng, G. Ungar, D. J. P. Yeardley, *J. Am. Chem. Soc.* **1998**, *120*, 8619. b) Y.-M. Chen, C.-F. Chen, W. H. Liu, Y. F. Li, F. Xi, *Macromol. Rapid Commun.* **1996**, *17*, 401. c) W. Stocker, B. Karakaya, B. L. Schürmann, J. P. Rabe, A. D. Schlüter, *J. Am. Chem. Soc.* **1998**, *120*, 7691. d) T. Sato, D. L. Jiang, T. Aida, *J. Am. Chem. Soc.* **1999**, *121*, 10658. d) S. Förster, I. Neubert, A. D. Schlüter, P. Lindner, *Macromolecules* **1999**, *32*, 4043. e) L. Shu, A. Schäfer, A. D. Schlüter, *Macromolecules* **2000**, *33*, 4321.
[11] a) M. L. Schilling, H. F. Katz, D. I. Cox, *J. Org. Chem.* **1988**, *53*, 5538. b) T. A. Chen, A. K.-Y. Jen, Y. Cai, *J. Am. Chem. Soc.* **1995**, *117*, 7295. c) T. A. Chen, A. K.-Y. Jen, Y. Cai, *Macromolecules* **1996**, *29*, 535. d) H. Ma, X. Wang, X. Wu, S. Liu, A. K.-Y. Jen, *Macromolecules* **1998**, *31*, 4049. e) J. Luo, J. Qin, H. Kang, C. Ye, *Chem. Mater.* **2001**, *13*, 927.
[12] J. S. Moore, S. I. Stupp, *Macromolecules* **1990**, *23*, 70.
[13] T. W. Greene, P. G. M. Wuts, *Protective Groups in Organic Synthesis*, 2nd ed., John Wiley & Sons, Inc., New York **1994**.
[14] S. S. Yoon, W. C. Still, *Tetrahedron* **1995**, *51*, 567.
[15] a) D. W. Smith Jr., D. A. Babb, *Macromolecules* **1996**, *29*, 852. b) D. W. Smith Jr., D. A. Babb, H. V. Shah, A. Hoeglund, R. Traiphol, D. Perahia, H. W. Boone, C. Langhoff, M. Radler, *J. Fluorine Chem.* **2000**, *104*, 109. c) H. Ma, J. Wu, P. Herguth, B. Chen, A. K.-Y. Jen, *Chem. Mater.* **2000**, *12*, 1187.
[16] C. C. Teng, H. T. Man, *Appl. Phys. Lett.* **1990**, *56*, 1734.
[17] H. E. Katz, C. W. Dirk, M. L. Schelling, K. D. Singer, J. E. Sohn, *Mater. Res. Soc. Symp. Proc.* **1987**, *109*, 127.
[18] C. Zhang, L. R. Dalton, M.-C. Oh, H. Zhang, W. H. Steier, *Chem. Mater.* **2001**, *13*, 3043.

Templating of Po
Porous Silica and

By *Ulrika Meyer, An*
and *Rachel A. Caruso*

Templating techniq
morphology of inor
films.[5] and hollow sp
organic structures ob
nipulate the structur
materials. The templ
the required morpho
matter. The mould i
precursor that covers
the precursor has re
species, the template
resembles that of t
formed nanoparticles
template, resulting in
niques allows the for
dimensions and morp
pore structuring and
such parameters pro
materials with novel
formance of the inor
sity of application.

The sphere with its
cations: The spherical
ties and is ideal for
Spherical beads that a
prove the properties
surface plus the adde

The use of porous
examined here for th
with porous inner st
have promising activi
catalysis, separation
example, in photocat
to dispersed nanopar
lyst from solution on
significant surface are
allowing contact of t
of inorganic surface.
meric bead morphol

[*] Dr. R. A. Caruso, Dr.
Max Planck Institute
D-14424 Potsdam (Ge
E-mail: Rachel.Caruso
U. Meyer, A. Larsson
Amersham Bioscience
Björkgatan 30, SE-751

[**] Prof. Markus Antoni
thank Rona Pitschke
with TEM analysis. T
Max Planck Society fo